J Mater Sci (2009) 44:2765–2773
DOI 10.1007/s10853-009-3361-7

Synthesis, characterization, and photochromic behaviors of polythiophene derivatives in the solid state

Bing-zhu Zhang · Xiong-yan Zhao

Received: 4 December 2008 / Accepted: 17 February 2009 / Published online: 9 March 2009

Abstract Novel polythiophene derivatives with azobenzene chromophore side chains, poly[3-(6-((4-phenylazo) phenoxyl)hexyl)thienylacetate] (PATh-6), and the copolymers of 3-(6-((4-phenylazo)phenoxyl)hexyl)thienylacetate with 3-alkylthiophenes including 3-hexylthiophene and 3-dodecylthiophene (COP-66 and COP-612) were synthesized. The structure and the thermal property of these polythiophene derivatives were characterized by NMR, FT-IR, UV–vis, XRD, GPC, MDSC, and TGA. The differences in photochromic features and thermochromic behaviors between homopolymer and copolymers have been comparatively studied. The photochemical control of photoluminescence property was achieved with homopolymer PATh-6 both in solution and in the solid state. However, this photo-induced effect becomes less prominent for copolymers COP-66 and COP-612 due to the lower content of azobenzene chromophore in the side chain of copolymers. The photo-induced photochromic feature of homopolymer PATh-6 might be promising for the development of novel field-responsive materials.

Introduction

Since conjugated polymers with delocalized π-electrons offer unique physical properties which are unobtainable for the conventional polymers, significant research efforts directed toward a better understanding of their chemistry, physics, and engineering have been undertaken in the last twenty years [1–3]. The greater part of the research study on heterocyclic conjugated polymers has centered on poly(thiophene)s [4–8], mainly because, by the introduction of a suitable side group, a variety of soluble derivatives of the polymer can be made. By a proper choice of the side group, optical and processing properties such as melting point and solubility can be tailored. One member of this family is the poly(3-alkylthiophene)s. The introduction of alkyl groups longer than butyl to the 3-position of the thiophene unit yields moderate-to-high molecular weight materials soluble in common organic solvents. The length of the alkyl side group affects melting point, conductivity etc. Moreover, the presence of substituents in 3-position can even lead to novel physical phenomena that are not found in the unsubstituted parent form. For example, the introduction of photochromic chromophore as a side group to the conjugated polythiophene backbone significantly alters electrochemical and spectroelectrochemical behavior [9] as well as conductivity [10] of these new polymers as compared to the corresponding parent forms. Furthermore, other successful attempts of polythiophene functionalization have also been achieved by the addition of functional side groups onto the aromatic backbones, such as redox-active groups [11, 12], mesogenic group [13], and photochromic groups [14], etc. These photoactive azobenzene-functionalized poly(thiophene)s have potential applications in the following areas: (1) the controller of conductivity [10], (2) field-responsive materials [15], (3) detector based on color change [16], (4) highly sensitive photochromic or affinity chromic materials [17]. Therefore, the synthesis of azobenzene-functionalized polythiophenes has attracted much interest both from synthetic considerations as well as from material science.

B.-z. Zhang
School of Chemical Engineering and Technology, Hebei University of Technology, Tianjin, People's Republic of China

B.-z. Zhang · X.-y. Zhao (✉)
College of Material Science & Engineering, Hebei University of Science and Technology, Shijiazhuang, People's Republic of China
e-mail: zhaoxy66@126.com

In a previous article by these authors [18], a series of azobenzene-functionalized thiophene copolymers have been synthesized and the structural dependence of thermochromic behavior of these copolymers was systematically investigated and results compared with poly(3-hexylthiophene) (P3HT). In this study, the differences in photochromism and thermochromism between azobenzene-functionalized thiophene homopolymer and azobenzene-functionalized thiophene copolymer have been comparatively studied by us with a special emphasis on photochromic features that originate from a combination of polythiophene backbone and azobenzene-containing side chain. It is well known that azobenzene chromophore was a kind of good photo-isomerizable unit [19–22] for reversible optical data storage and other electro-optic devices. Thus, the combination of polythiophene backbone with photoactive azobenzene groups could provide a new approach to develop other novel materials with unique electronic and optical properties. It has been reported that there is a strong correlation between the electronic structure and the backbone conformation for conjugated polymers; the introduction of photoactive groups to polythiophenes is therefore expected to be favorable from the viewpoint of control of the photoluminescence property. Following this guidance, a series of polythiophene derivatives with photoactive azobenzene as side chains were synthesized (see Scheme 1), the synthesis and characterization and the structure–property relationship of these azobenzene-functionalized polythiophenes were also discussed.

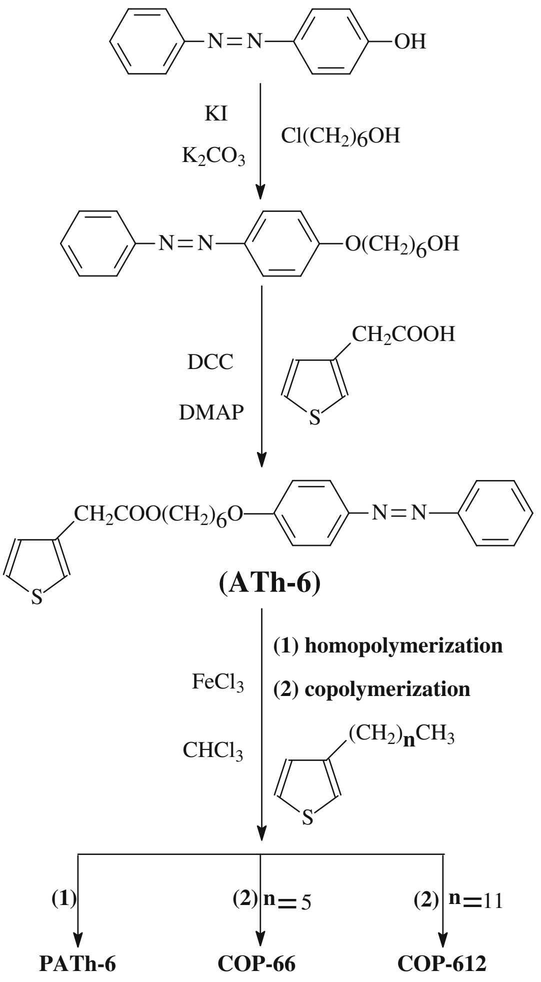

Scheme 1 The synthesis scheme of azobenzene-functionalized polythiophenes

Experimental details

Synthesis

Synthesis of 4-(6-hydroxyhexyloxy)azobenzene (HHAB)

To a 250-mL three-neck round flask containing 100 mL of anhydrous dimethyl sulfoxide, 5.5 g (27.7 mmol) of 4-phenylazophenol and 7.15 mL (53.5 mmol) of 6-chloro-1-hexanol were added, and then, 0.20 g of potassium iodide (catalyst) and 7.5 g (54.5 mmol) potassium carbonate were added. The reaction system was magnetically stirred and maintained at 110 °C by an oil bath for about 8 h. The reaction solution was cooled to room temperature and the salts were filtered out with a Buchner funnel. The filtrate was poured into a fourfold volume of ice-cold water and stirred for a while, then allowed to settle for overnight. The precipitate collected was washed with water for several times, and then it was recrystallized in methanol twice. This reaction gave a yellow powder with a melting point of 76.5 °C. FT-IR (KBr, cm^{-1}): 3288 (–OH); 3065 (Ar; =CH); 2861, 2935 (aliphatic; ν_s and ν_{as} of –CH_2–); 1603, 1584, 1474 (Ar; C=C); 1500, 1442 (N=N; *cis* and *trans*); 1254; (C–O–C; ν_{as}); 1070 (C–O–C; ν_a); 841 (Ar; =CH; *p*-substituted benzene ring); 686, 764 (Ar; =CH; mono-substituted benzene ring). ^{1}H NMR ($CDCl_3$, 400 MHz, ppm): 1.48 (broad, OH), 1.50–1.57 (m, 3H), 1.64 (q, 3H), 1.86 (t, 2H), 3.70 (t, 2H), 4.07 (t, 2H), 7.02 (t, 2H), 7.46 (d, 1H), 7.52 (q, 2H), 7.92 (m, 4H). Anal. Calcd. for $C_{18}H_{22}N_2O_2$: C, 72.48; H, 7.38; N, 9.41; O, 10.73. Found: C, 72.50; H, 7.35; N, 9.40.

Synthesis of 3-(6-((4-phenylazo)phenoxyl)hexyl) thienylacetate (ATh-6)

A total of 0.97 g (6.8 mmol) of 3-thiopheneacetic acid (Aldrich) and 1.60 g (5.4 mmol) of HHAB were dissolved in 80 mL of dry CH_2Cl_2. The solution was cooled down to 0–5 °C with ice-water bath, to which 1.44 g (7.0 mmol) dicyclohexylcarbodiimide (DCC) (Aldrich) and 0.12 g (1.01 mmol) of dimethylaminopyridine (DMAP) (Aldrich) were added to the vigorously stirred solution. The reaction mixture was stirred overnight. After filtering out the urea solid formed, the solution was concentrated using a rotary evaporator under vacuum. The product was purified by the silica gel column chromatography using chloroform as the eluant. This reaction gave a yellow crystal with a melting point of 87.6 °C. FT-IR (KBr, cm^{-1}): 3099 (Ar; =CH); 2866, 2942, 2961 (aliphatic; $–CH_2–$); 1740 (C=O); 1607, 1583, 1473 (Ar; C=C); 1504, 1443 (N=N; *cis* and *trans*); 1260; (C–O–C; ν_{as}); 1070 (C–O–C; ν_a); 842 (Ar; =CH; *p*-substituted benzene ring); 687, 770 (Ar; =CH; monosubstituted benzene ring). ^1H NMR ($CDCl_3$, 400 MHz, ppm): 1.53 (m, 3H), 1.70 (t, 3H), 1.84 (t, 2H), 3.67 (d, 2H), 4.06 (t, 2H), 4.15 (t, 2H), 7.03 (d, 2H), 7.06 (s, 1H), 7.29 (t, 2H), 7.45 (s, 1H), 7.51 (t, 2H), 7.91 (m, 4H). Anal. Calcd. for $C_{24}H_{26}N_2O_3S$: C, 68.25; H, 6.16; N, 6.64; S, 7.58; O, 11.37. Found: C, 68.26; H, 6.13; N, 6.61; S, 7.55.

Synthesis of poly[3-(6-((4-phenylazo)phenoxyl)hexyl)thienylacetate] (PATh-6)

The polymerization was carried out in a baked 25-mL Schlenk reaction flask with glass stopcock on the side arm under the constant flow of dry argon. The typical synthesis procedures utilized can be described as follows: 0.44 g (2.72 mmol) of anhydrous $FeCl_3$ was quickly put into the flask, which was subsequently evacuated and flushed with argon three times. Then, 5 mL of anhydrous $CHCl_3$ was syringed into the reaction vessel at 0–5 °C followed by the addition of 0.25 g (0.59 mmol) monomer in 3 mL $CHCl_3$ dropwise for 30 min. After the entire monomer was added into the flask, the reaction mixture was stirred at the room temperature for 5 h. The polymerization reaction was terminated by pouring the reaction mixture into 200 mL methanol. The precipitated polymer was then washed repeatedly with water and methanol, and dedoped in aqueous ammonia. Finally, the polymer was further purified in a Soxhlet apparatus with methanol for 24 h. $Mw = 2.28 \times 10^4$, $Mw/Mn = 3.01$.

Synthesis of copolymer of 3-(6-((4-phenylazo)phenoxyl)hexyl)thienylacetate with 3-hexylthiophene (COP-66)

The copolymerization was carried out by seed-polymerization method using anhydrous $FeCl_3$ as catalyst. In a 50-mL Schlenk reaction flask, 0.9 g (5.5 mmol) of anhydrous $FeCl_3$ was quickly introduced, which was subsequently evacuated and flushed with argon three times. Then, 15 mL of anhydrous $CHCl_3$ was syringed into the reactor at 0–5 °C followed by the addition of 0.2 g (0.48 mmol) monomer in 3 mL $CHCl_3$ in one portion. After a certain period of time, a solution of 3-hexylthiophene (3HT) in 5 mL of $CHCl_3$ was added in dropwise manner for 20 min. Then, the reaction mixture was stirred at the room temperature for another period of time. The polymerization reaction was terminated by the addition of 200 mL of methanol. The precipitated polymer was then washed repeatedly with water and methanol, and dedoped in aqueous ammonia. Finally, the copolymer was further purified in a Soxhlet apparatus with methanol for 24 h. $Mw = 6.56 \times 10^4$, $Mw/Mn = 1.60$.

Synthesis of copolymer of 3-(6-((4-phenylazo)phenoxyl)hexyl)thienylacetate and 3-dodecylthiophene (COP-612)

COP-612 was synthesized using the same synthetic procedure as for COP-66. $Mw = 5.73 \times 10^4$, $Mw/Mn = 1.62$.

Characterization

An S-4800 Scanning electron microscope (SEM) was used to examine the surface structure of the polymer thin films obtained. NMR spectra were recorded on a BRUKER 400 NMR spectrometer at 400 MHz in deuterated chloroform with TMS as an internal standard. The elemental analyses were performed using a Mitamura Riken Kogyo@ micro-elementary analyzer. Differential scanning calorimetry (DSC) analyses were performed at 5 °C/min on a TA instrument using Modulated DSC (model Q-200). Thermal stability measurements were carried out on a Hi-Res TGA 2950 thermogravimetric analyzer under a nitrogen flow at a heating rate of 10 °C/min. The molecular weights of the samples were measured by gel permeation chromatography (GPC, waters 410; eluant, THF) calibrated with monodispersed polystyrene standards. X-ray diffractions of polymer films on glass slides were measured using a Rigaku Rint 2000 X-ray Diffractometer and operated at 40 kV, 30 mA, and the data were collected from 1.5 to 40° (2θ) at a scan rate of 2°/min. FT-IR spectra were recorded on a Perkin-Elmer System 2000 FT-IR spectrometer. The compound and monomer were prepared as KBr pellets, and the polymers were deposited on the surface of KBr disks by casting from chloroform solutions, which were then dried under an IR lamp for 5 min, and the spectra were taken. UV–visible spectra were obtained using an UV–vis recording spectrophotometer (Shimadzu, Model UV-2501PC). For the solid-state measurements, the spectrophotometer was provided with a temperature control unit that allows measurements over a temperature range 25–250 °C with a maximum error of ±2 °C. Fluorescence measurements were conducted on a Shimadzu RF5000 spectrofluorophotometer. The photochromic experiments were carried out using an ARC lamp (Oriel, Model 68910, 500W) as the light source. The monochromatic light that peaked at 362 and 410 nm was isolated using filter (Model 58650 and 59285). The polymer powders were dissolved in the appropriate solvents (e. g., CH_3Cl) and then allowed to settle for 24 h in the dark before irradiation. To prepare thin films, the polymer was dissolved in chloroform, filtered, and then the solution was deposited by spin-coating method at a speed of 2000 rpm for 10 s, onto clean quartz slides, and finally dried under vacuum for 24 h.

Results and discussion

From the ^{1}H NMR results of PATh-6, we can assign the following peaks to PATh-6: 1.52 ($–(CH_2)_4–$), 3.58, 3.78 ($–CH_2–COO–$), 3.94 ($–CH_2–O–Ar$), 4.12 ($–COO–CH_2–$), 6.94, 7.47, 7.86 (protons of phenylene rings), 6.92 (β'-proton of thiophene ring). The small peak located around 7.12 is not well resolved and has multiplet splitting, which is due to the β'-proton of the thiophene ring for various regioisomeric units in the polymer chain [23]. Previous reports have shown that the oxidative polymerization of β-substituted thiophene monomer with ferric chloride always led to two different types of couplings: head-to-tail and head-to-head [24–27]. Thus, the α-methylene protons directly attached to the thiophene ring (β-position) can be incorporated into a polymer chain with above two diads. The two peaks located at 3.58 and 3.78 ppm arise from the methylene protons between the ester group and the thiophene ring [10], which show that PATh-6 has a stereo-random chain structure with almost equal distribution of head-to-tail and head-to-head linkages along the polymer chain.

The chemical structure of both copolymers was also analyzed by ^{1}H NMR. On the basis of the comparison between the spectra of the two monomers, the following assignments corresponding to the protons of 3-hexylthiophene unit can be given: 0.93 ($–CH_3$), 1.36, 1.45 ($–CH_2CH_2CH_2–Me$), 1.61, 1.71 (β-CH_2–) [24], 2.56, 2.82 (α-CH_2–) [27]. The peaks assigned to the ATh-6 unit are as follows: 1.36, 1.45 ($–(CH_2)_4–$), 3.58, 3.79 ($–CH_2–COO–$), 4.18 ($–COO–CH_2–$), 3.96 ($–CH_2–O–Ar$), 7.00, 7.48, 7.87 (protons of phenylene rings), The peak at 7.00 ascribable to the β'-proton of thiophene ring of both ATh-6 and 3-HT units overlaps with that associated with the phenylene ring. The ^{1}H NMR signals at $\delta = 2.56$ and 2.82 ppm correspond to the α-CH_2– group of the 3-hexylthiophene unit for the head-to-head and head-to-tail coupling, respectively. The intensities of these two peaks suggest the presence of about 23% of head-to-head coupling of the 3-hexylthiophene units in the copolymer. Similarly, the peaks at $\delta = 3.58$ and 3.79 ppm correspond to the α-CH_2– group of ATh-6 unit for the head-to-head and head-to-tail coupling, respectively. The intensities of these two peaks indicate equal distribution of head-to-head and head-to-tail linkages among ATh-6 units. Furthermore, the small but distinct peak at 3.48 ppm is suggested to be due to the α-CH_2– units of the mixed coupling between the ATh-6 unit and a 3-hexylthiophene-unit [23]. Variations in configuration and location of some peaks of ATh-6 unit in copolymer COP-66 as compared with those of homopolymer PATh-6 indicate that the adjacent structure and chemical environment of some protons have been changed, which supports the formation of copolymer.

Figure 1 illustrates the FT-IR spectra of PATh-6, COP-66, and COP-612, along with spectrum of the azobenzene-attached thiophene monomer (ATh-6). The polymerization process of ATh-6 has been confirmed by the disappearance of the band at 732 cm^{-1}, which is attributable to C–Hα out-of-plane deformation vibration of thiophene rings. Moreover, the existence of the following bands further confirmed the formation of homopolymer PATh-6: 3073 (Ar; =CH); 2855, 2927 (aliphatic, $–CH_2–$); 1736 (C=O); 1601, 1581, 1468 (Ar, C=C); 1502, 1442 (N=N, *cis* and *trans*); 1251 (C–O–C, ν_{as}); 1069 (C–O–C, νa); 838 (Ar, =CH, *p*-substituted benzene ring); 686, 765 (Ar, =CH, mono-substituted benzene ring). For the copolymers COP-66 and COP-612, spectral features of the ester derivatives of ATh-6 are clearly seen in both the copolymers' spectra, especially with the bands occurring at 1735 and 1251 cm^{-1}, respectively, which can be ascribable to carbonyl (C=O) stretching vibration and C–O–C stretching vibration (ν_{as}) respectively. Furthermore, the absorption bands occurring at 1377 cm^{-1} ($–CH_3$, δ_s deformation vibration) and 2954 cm^{-1} ($–CH_3$, ν_{as} stretching vibration) in copolymers are characteristic of 3-alkylthiophene blocks, thus the FT-IR data of this study support the

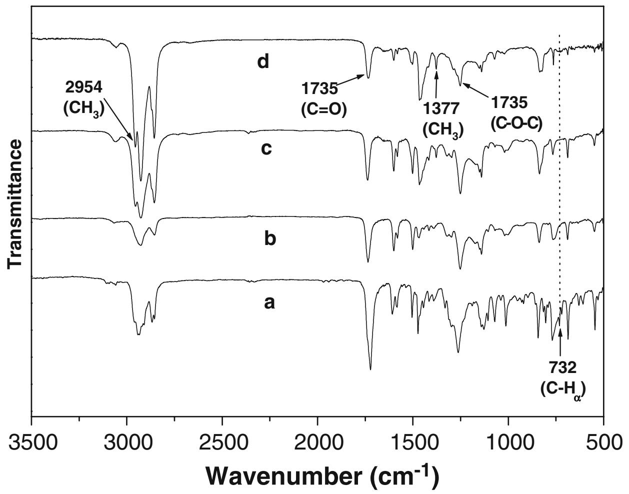

Fig. 1 FT-IR spectra of (a) Monomer ATh-6, (b) PATh-6, (c) COP-66, and (d) COP-612

existence of ATh-6 and 3-alkylthiophene segments in copolymer. It is necessary to mention that some of the FT-IR bands associated with the polythiophene backbone strongly superimpose with those originating from the photoactive chromophore. For example, the peak at 832 cm^{-1} (Ar; =CH, *p*-substituted benzene ring) in azobenzene is very close to the peak at 827 cm^{-1} associated with the out-of-plane C–H_β deformation vibration of thiophene rings, which is characteristic of 2,3,5-trisubstituted thiophene ring.

X-ray diffraction patterns of the polymer and copolymer films on glass slide cast from chloroform solution are shown in Fig. 2. For comparison, the spectrum of poly (3-hexylthiophene) (P3HT) is also presented in Fig. 2.

For PATh-6, after scanning from 1.5 to 40°, only a very broad, single. diffused scattering peak with a maximal intensity at around 21° is observed, indicating that no crystalline can be observed by the X-ray diffraction and that there exists a broad distribution of intraplanar and interplanar distance [28]. For both copolymers, in addition to a broad amorphous peak at wide angle, two separate diffraction peaks also appeared at low angle: a very intensive peak with a maximum intensity around at 5.19°, and a small but distinct diffraction peaks around at 10.5°. It is interesting to note that the d spacing change is less prominent with an increase in the length of the 3-alkylthiophene segments in copolymer (see Table 1). This could be attributed to the presence of bulkier chromophore group which.offsets the effect of side chain length on the space filling of the side chain. Furthermore, the crystallinity of both copolymers is lower than that of P3HT as indicated by the less sharp diffraction peak in the XRD spectrum. In contrast with the case of P3HT, in which three orders of reflection were present at low-angle region with maxima at 5.25°, 10.6°, and 15.9°, respectively (see Fig. 2d), only the first- and second-order reflections of the copolymer samples were observed. This reveals that a lower degree of space filling of the side chains exists in copolymers than in P3HT [29] probably due to the presence of bulky chromophore groups and more polar carbonyl groups which hinder the intercalation of the side chains.

Table 1 X-ray diffraction 2θ positions and calculated *d* spacing

Samples	2 θ (°)/*d* spacing (Å)			
	Low angle			Wide angle
	First	Second	Third	
PATh-6	–	–	–	–
COP-66	5.19/17.0	10.6/8.3	–	–
COP-612	5.19/17.0	10.5/8.4	–	–
P3HT	5.25/16.9	10.6/8.3	15.9/5.6	21.3/4.2

The thermal stability of the three polymers was investigated under a nitrogenatmosphere at a heating rate of 10 °C/min. Figure 3 presents the TGA curves of PATh-6, COP-66, and COP-612. In addition, the TGA trace of P3HT is also illustrated as a comparison. PATh-6 and COP-66 depict two obvious weight-loss steps in the temperature range of 30–800 °C, and COP-612 exhibits two, though not completely, distinct weight-loss steps as indicated by the derivative weight curve. The first step corresponds to the loss of azobenzene-containing side chain and the second one can be ascribable to the degradation of the alkyl side chain and polymer backbone. The initial decomposition temperature of PATh-6, COP-66, and COP-612 is found to be lower than that of P3HT which is stable up to 400 °C, as can be seen from Table 2. This can be attributed to the presence of polar pendant side chains in these polymers that make the polymer system more reactive and be more easily oxidized.

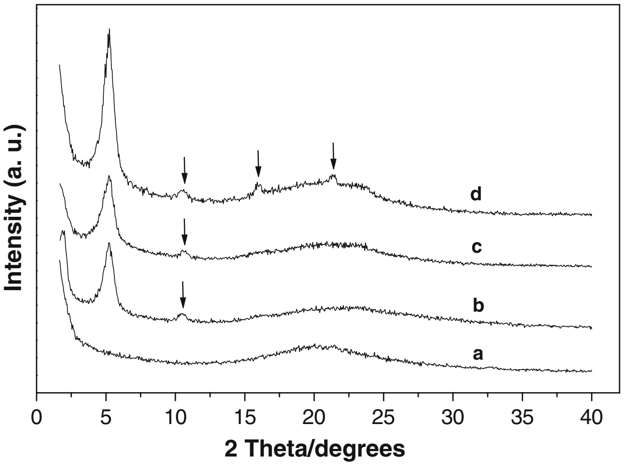

Fig. 2 X-ray diffraction patterns of polymer films cast from chloroform solutions: (a) PATh-6, (b) COP-612, (c) COP-66, and (d) P3HT

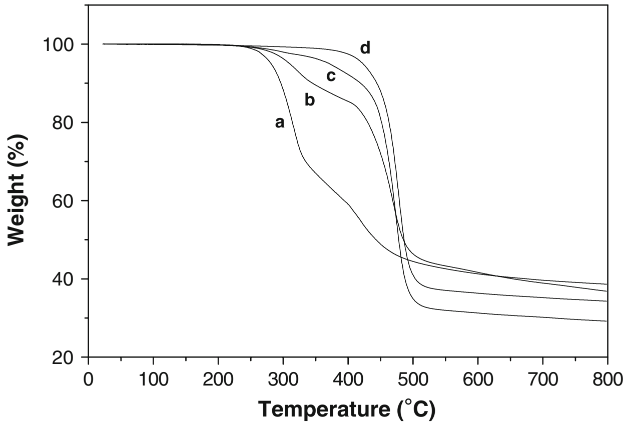

Fig. 3 TGA thermograms of (a) PATh-6, (b) COP-66, (c) COP-612, and (d) P3HT

Table 2 Thermal properties of polythiophene derivatives from TGA and MDSC

Polymers	Weight loss (%)		T_d (°C)	T_g (°C)	T_m (°C)
	1 st step	2 nd step			
PATh-6	36.9	22.9	270.8	30.2	–
COP-66	13.0	51.1	292.9	8.8	185.3
COP-612	8.24	60.9	332.4	−11.7	195.1
P3HT	63.4	–	400.5	4.3	192.6

Modified differential scanning calorimetry (MDSC) can provide a better insight into the study of complicated transition in polymers. All the MDSC runs in this research were made under a nitrogen atmosphere with heating and/or cooling rates of 5 °C/min. The MDSC results (glass transition temperature T_g and melting temperature T_m) are also listed in Table 2. As a result of heating from −30 to 250 °C, COP-66, and COP-612 displayed two apparent transitions as indicated by the reversing heat flow curves, corresponding to the glass transition temperature, T_g, and the melting temperature, T_m, of the two copolymers. For homopolymer PATh-6, however, only one transition at 30.2 °C appeared during the heating scan, which is assigned to the glass transition. This further confirms the amorphous structure of PATh-6. These results reveal that both copolymers have a much higher ordered phase as compared with PATh-6. And they also indicate that the flexible alkyl side chain can provide a higher free volume, allowing the molecular chains to realign more easily than the rigid side chain, which are agreeing well with the XRD results.

The morphologies of PATh-6 and COP-66 films deposited on quartz slides using spin-coating method were observed using SEM. The SEM micrographs in Fig. 4 show that high quality PATh-6 film (Fig. 4a) and COP-66 film (Fig. 4b) could be obtained. They are transparent, homogeneous, and pinhole-free, suitable for the measurement of photochromic and thermochromic properties.

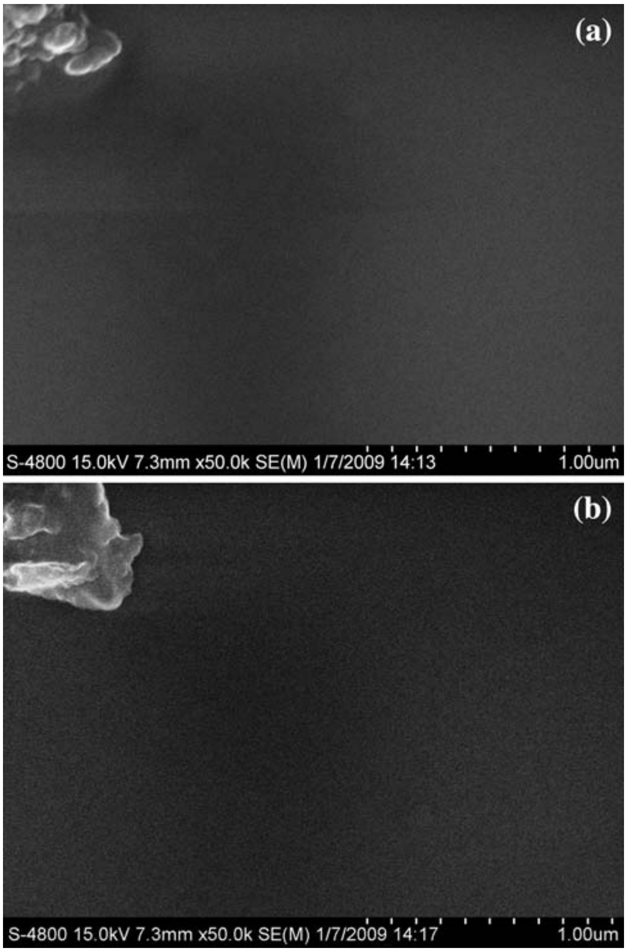

Fig. 4 Surface morphology of polymer films measured by SEM: **a** PATh-6, and **b** COP-66

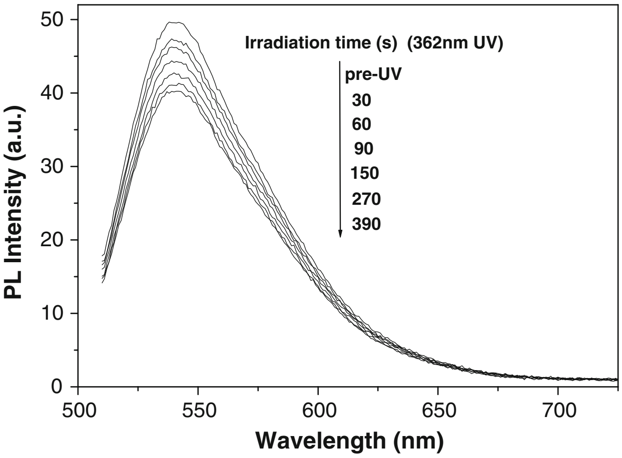

Fig. 5 Photoluminescence spectra of PATh-6 in chloroform for a 498-nm-excitation wavelength with different UV irradiation time at 362 nm

The effect of photo-isomerization of photoactive azobenzene side chain on photoluminescence properties of polythiophene main chain was also investigated. It has been reported that [10] the photons can be absorbed entirely in the surface region of less than 1 μm because of the much larger molar extinction coefficient of the π–π^* transition of the azobenzene chromophore at about 360 nm. The polymer thin films with a thickness less than 300 nm were used in order to allow complete photochemical reaction across the films. Due to irradiation by the UV light of 362 nm, the intensity of fluorescence of PATh6 in chloroform was found to decrease with UV irradiation (Fig. 5), and this photochromic behavior was also observed for PATh6 sample in the solid state (Fig. 6). These results indicate that the optical property of the azobenzene-functionalized polythiophene might be controlled by the photo-induced isomerization of the photoactive groups covalently attached

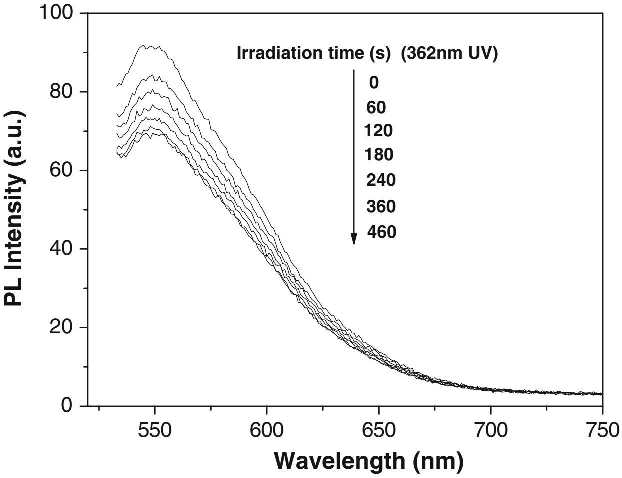

Fig. 6 Photoluminescence spectral changes of PATh-6, as a function of time of UV irradiation (362 nm), in the solid state (excited at 538 nm)

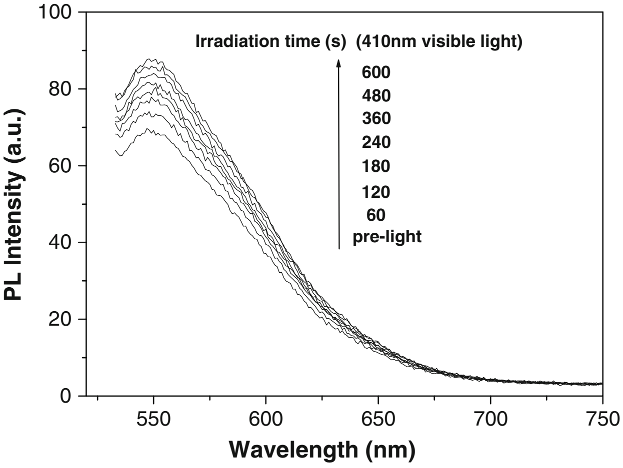

Fig. 7 Photoluminescence spectral changes of PATh-6, as a function of time of visible light irradiation (410 nm), in the solid state (excited at 538 nm)

to the thiophene rings. For practical applications as photochromic materials, it could be interesting to investigate the reversible photochromic behaviors in the solid state. As shown in Fig. 7, when the irradiated samples were irradiated by the visible light of 410 nm, the intensity of fluorescence steadily increased to a value close to the starting value before irradiation. Thus, the photoresponsive polythiophene synthesized in this research might be a promising material used as field-responsive material for completely new applications such as photodetector. For copolymer COP-66, however, the emission intensity change is less prominent during UV irradiation (Fig. 8). Similar result was also observed for the copolymer COP-612. It is well known that the properties of *cis*-azobenzene are very different from those of *trans*-azobenzene. For an

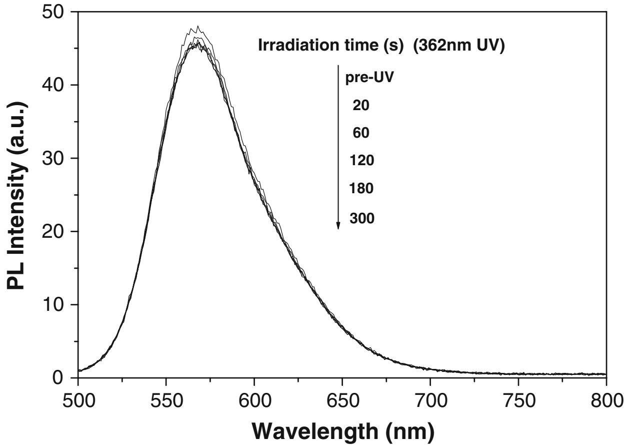

Fig. 8 Photoluminescence spectra of COP-66 in chloroform for a 535-nm-excitation wavelength with different irradiation time at 362 nm

unsubstituted azobenzene, when the linear *trans*-isomers changes to the bent *cis*-isomers, the distance between the *para*-carbon atoms decreases from 9 to 5.5 Å, and the dipole moment increases from zero to 3.0 D. Thus, the *trans–cis* photoisomerization will bring about a structural rearrangement in the azobenzene side chains, producing steric pressure and electronic interactions that could force changes in the conformation of polymer main chain. The torsion angle between the thiophene rings of main chain decreases with the reorganization of azobenzene chromophore side chains, which will result in an increase of the overlapping of the neighboring p_z atomic orbital, and finally leads to an increase in the degree of conjugation (coplanarity) of polythiophene backbone. The proposed conformational changes of polythiophene backbone during UV irradiation are shown in Fig. 9. It has been reported that the twisted form of the conjugated polymer backbone shows fluorescence whereas the planar form does not emit at all [30, 31]. It has been suggested that the conformational defects (a twisted conformation) can act as traps for energy migration and therefore inhibit nonradiative decay [32, 33]. The increase in coplanarity of the thiophene rings caused by photo-induced isomerization of pendent azobenzene chromophore will thus bring about the enhancement of nonradiative decay of excited species [31, 33]. Hence, the photoluminescence intensity of PATh6 decreases with the increase of UV irradiation time. For copolymer COP-66 and COP-612, the smaller change in fluorescence intensity with the photoisomerization of azobenzene chromophore can be attributed to the lower content of chromophore in the side chain of copolymer which is too low to induce distinct change in coplanarity of polythiophene backbone.

Since the strong blue shift in the absorption maximum in the visible region can take place with the thermally induced

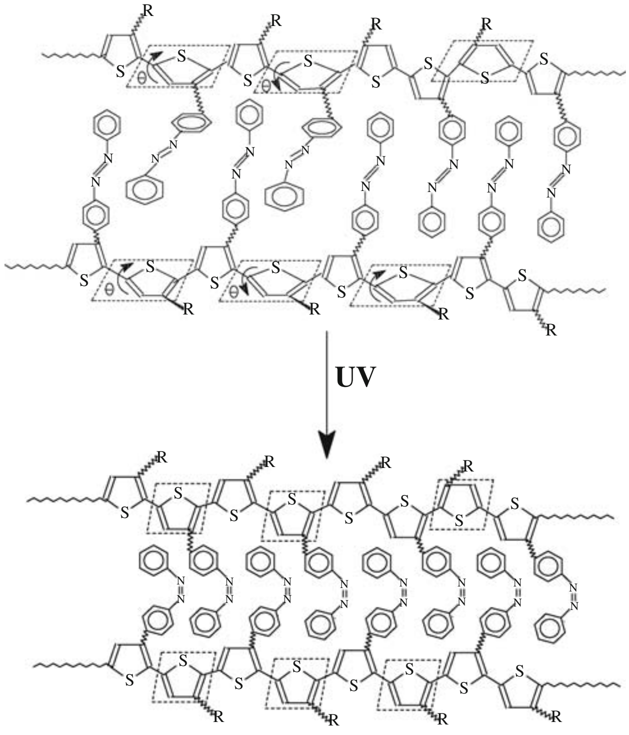

(**R**=azobenzene or hexyl group)

Fig. 9 The proposed conformational changes of polythiophene backbone during UV irradiation

disordering of the side chains of polythiophenes, these thermochromic polymers can be useful not only as optical temperature indicators but also as materials for thermal recording. The thermochromic behaviors of all the polymers obtained in this study were evaluated by heating UV–vis absorption measurements. It is clear from Fig. 10 that no thermochromism was observed for homopolymer PATh-6 in addition to small variations in band absorption intensity caused by thermal *cis–trans* isomerization. This can be attributed to the excess number of rigid azobenzene groups present in the side chains and also the existence of more polar carbonyl groups. It is known that [34, 35] the thermochromic phenomenon results from a delicate balance between repulsive side chains steric interactions and attractive interchain interactions with the latter interactions being necessary to stabilize the low-temperature planar conformation. Since the strong side-chain steric interactions between PATh-6 molecules, no planar (or nearly planar) conformation is accessible for this polymer at the room temperature. Therefore, no thermally induced planar-to-nonplanar conformational transition can take place. For copolymer COP-612, however, due to the introduction of thiophene segments with highly flexible and less polar alkyl side chains, a quite obvious reversible thermochromic effect has been observed in the solid state (Fig. 11). It is clear from Fig. 11 that as a result of heating, COP-612 film exhibits an obvious blue shift and a clear isosbestic point is also observed, revealing the cooperative twisting of the azobenzene-functionalized polythiophene backbone. Moreover, this absorbance change is fully reversible, and, upon cooling, the copolymer films can recover their initial absorption spectra. Similar result was also observed for copolymer COP-66. This strong dependence of the thermochromic properties upon the type of substituents can be explained by a cooperative formation of intramolecular and intermolecular assemblies, which would be reversibly broken through thermally induced side chain disordering. It is believed that a better understanding of the structure–property relationships can be not only useful for the improvement of the physical properties of polythiophenes but also helpful for the rational design of novel polythiophene derivatives.

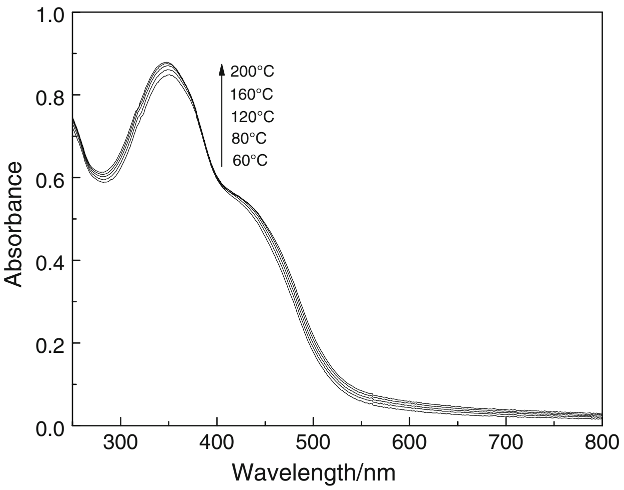

Fig. 10 Temperature-dependent UV-visible spectra of PATh-6 in the solid state

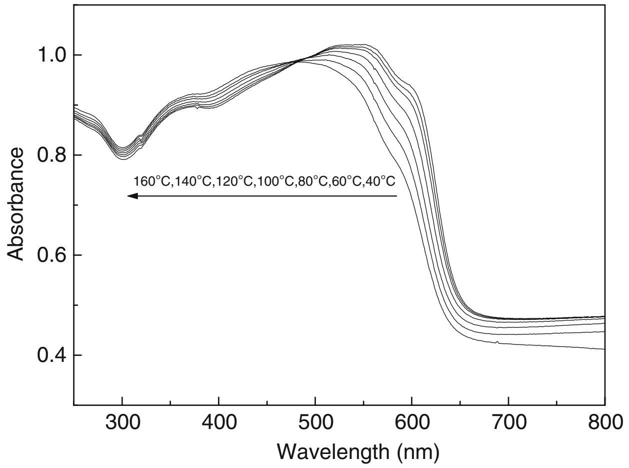

Fig. 11 Temperature-dependent UV-visible spectra of COP-612 in the solid state

Conclusion

In this research, a series of polythiophene derivatives with photoactive azobenzene groups have been synthesized and characterized. It was found that the photoluminescent features associated with the conjugated backbone of homopolymer PATh-6 can be reversibly controlled through a photo-induced isomerization reaction of photoactive azobenzene side chains. In the case of copolymers COP-66 and COP-612, however, the photochemical isomerization of photoactive groups in the side chains showed only a quite limited effect on photoluminescent property, which indicates that the *trans–cis* isomerization of the azobenzene group in order to induce the structural change in the polythiophene backbone has diminished in copolymers because of the lower content of photoactive chromophore in the side chain. Furthermore, an obvious reversible thermochromic effect has been observed for both copolymers in the solid state when thiophene units with highly flexible and less polar hexyl side chains were introduced into polymer chains. Thus, it is clear that although the optical transitions are obviously related to conformational changes of the conjugated backbone, it seems that the polymer structure, such as the nature of the substituents, has a strong influence on the conformation and the optical properties of the resulting polythiophene derivatives.

Acknowledgments The project was sponsored by the Scientific Research Key Foundation for Returned Overseas Chinese Scholars, Ministry of Personnel of the People's Republic of China. This project was also supported by the Natural Science Foundation of Hebei Province (B2007000613), and by the Research Fund of Hebei University of Science and Technology.

References

1. Pron A, Rannou P (2002) Prog Polym Sci 27:135
2. Saxena V, Malhotra BD (2003) Current Appl Phys 3:293
3. Friend RH (2001) Pure Appl Chem 73:425
4. Woo CH, Thompson BC, Kim BJ, Toney MF, Fréchet JMJ (2008) J Am Chem Soc 130:16324
5. Osaka I, McCullough RD (2008) Acc Chem Res 41:1202
6. Osaka I, Sauvé G, Zhang R, Kowalewski T, McCullough RD (2007) Adv Mater 19:4160
7. Sauve G, McCullough RD (2007) Adv Mater 19:1822
8. Reeves BD, Unur E, Ananthakrishnan N, Reynolds JR (2007) Macromolecules 40:5344
9. Zagorska M, Kulszewicz-Bajer I, Pron A, Sukiennik J, Raimond P, Kajzar F, Attias AJ (1999) Synth Met 102:1141
10. Mochizuki H, Nabeshima Y, Kitsunai T, Kanazawa A, Shiono T, Ikeda T, Hiyama T, Maruyama T, Yamamoto T, Koide N (1999) J Mater Chem 9:2215
11. Ofer D, Crooks DM, Wrighton MS (1990) J Am Chem Soc 112:7869
12. Thobie-Gautier C, Gorgues A, Jubault M, Roncali J (1993) Macromolecules 26:4094
13. Thobie-Gautier C, Bouligand Y, Gorgues A, Jubault M, Roncali J (1994) Adv Mater 6:138
14. Yassar A, Moustrou C, Korri Youssoufi H, Samat A, Guglielmetti R, Garnier F (1995) Macromolecules 28:4548
15. Zagorska M, Kulszewicz-Bajer I, Pron A, Sukiennik J (1998) Macromolecules 31:9146
16. Levesque I, Leclerc M (1997) Synth Met 84:203
17. Levesque I, Leclerc M (1997) Macromolecules 30:4347
18. Zhao XY (2005) J Mater Sci 40:3423. doi:10.1007/s10853-005-2849-z
19. Buffeteau T, Lagygne LF, Pezolet M, Sourisseau C (1998) Macromolecules 31:7312
20. Berg RH, Hvilsted S, Ramanujam PS (1996) Nature 383:506
21. Maxein G, Zentel R (1995) Macromolecules 28:8438
22. Natansohn N, Rochon P (1999) Adv Mater 11:1387
23. Chittibabu KG, Li L, Kamath M, Kumar J, Tripathy SK (1994) Chem Mater 6:475
24. Yamamoto T, Komarudin D, Arai M, Lee BL, Suganuma H, Asakawa N, Inoue Y, Kubota K, Matsuda H (1998) J Am Chem Soc 120:2047
25. Barbarella G, Bongini A, Zambianchi M (1994) Macromolecules 27:3039
26. McCullough RD, Lowe RD, Jayaraman M, Anderson DL (1993) J Org Chem 58:904
27. Chen TA, Wu X, Rieke RD (1995) J Am Chem Soc 117:233
28. Miller RL, Boyer RF (1984) J Polym Sci Polym Phys Ed 22:2021
29. Chen SA, Ni JM (1992) Macromolecules 25:6081
30. Levesque I, Leclerc M (1996) Chem Mater 8:2843
31. Rughooputh SDDV, Bloor D, Phillips D, Movaghar B (1987) Phys Rev B 35:8103
32. Linton JR, Frank CW, Rughooputh SDDV (1989) Synth Met 28:C399
33. Yoshino K, Nakajima S, Onoda M, Sugimoto R (1989) Synth Met 28:C349
34. Leelerc M, Faid K (1997) Adv Mater 9:1087
35. Roux C, Bergeron JY, Faid K (1993) Makromol Chem 194:869